Angola Cameia Development Casing Settlement Calculations

J. Ed Akin, SPE, Rice University

N. Roland Dove, SPE, Ken Ruddy, SPE, Cobalt International Energy Incorporated

Houston, TX

Summary

The amount of axial settlement of casings supported by regions of axial elastic foundations is computed. The differential equation of axial equilibrium, including the foundation stiffnesses, is solved using cubic axial finite elements. The analysis is applied to 101 meters of a vertical 914 *mm* casing supporting a 559 *mm* casing running from three meters above the mudline to near the bottom of the 1201 meter hole. The upper casing is supported by a region of layered clay sediments. The lower casing has a long open hole region, followed by a bottom region encased in cement. A series of loading increments are applied, with the connection of the Tree/BOP being last. The settlement at the mudline was calculated to be less than 0.1 meter. This study shows that for weak upper foundations a good cement job is needed to support the Tree/BOP without large mudline settlements.

Introduction

Anderson (1984) reported that a cemented wellhead subsided by 0.71 *m* occurred while attempting to hang-off the production tubing. There have been past incidences when an installed sub-sea casing system was loaded with a Tree/BOP and was observed to sink below the mudline, resulting in well lost. New regulations have been proposed to address that possibility and to prevent it from happening in the future. Basically, under certain conditions those regulations require that a well be abandoned and a new well spudded. If that happens, the drilling company clearly suffers a large financial loss. The question addressed here is, what is the likelihood that the Angola Development casing system could sink below the mudline when its Tree/BOP is added? That in part depends on how much the axial elastic foundations at the top and bottom of the system contribute to the equilibrium of the system. An axial elastic foundation contributes an additional stiffness matrix to the portions of the casing surface that it contacts. An elastic foundation is quantified by the value of its "subgrade modulus". The subgrade modulus is defined as the force acting on a specified surface area required to displace that surface a specified amount in the direction of the force. It is usually specified with units of stress per unit length.

For the Angola casing installation all of the data are known except for the foundation subgrade modulus, *k*. The ASTM standard for measuring the foundation modulus is to use a standard punch to indent the foundation by a standard distance. The load, in Newtons, required causing that indentation, divided by the punch displaced volume, is the value of the foundation modulus in $N/m^2/m$ and its units are normally reported as N/m^3. The preferred English unit is *lb./in^2/in* or *psi/in* since *lb./in^3* could be confused with the foundation's specific weight. The reported subgrade modulus values vary greatly for various lithologies. It is not unusual to find the ratio of maximum over minimum values in the range of four or more. This implies that the present settlement estimate formulation should consider multiple estimates if experimental values of *k* cannot be supplied. The Appendix discusses foundation subgrade modulus values in more detail.

The details of the casing system are shown in **Fig. 1**. The upper 914 *mm* (36 *in.*) casing is supported by tertiary layers of sand and layers of clay sediments that form an axial elastic foundation. Those sediments are assumed to have a foundation modulus of 40.7e6 *N/m^2/m* (150 *lb./in^2/in*). Likewise, the encasing cement functions as an axial elastic foundation for the distal end of the lower 559 *mm* (22 *in.*) casing. The cement is assumed to have a foundation modulus of 81.4e6 *N/m^2/m* (300 *lb./in^2/in*). Typical foundation subgrade moduli values are discussed in the Appendix. The cement is assumed to begin at 886.4 *m* (2,908 *ft*) below the mudline and continue to the bottom of the casing at 1186.4 *m* (3,892.4 *ft*). That corresponds to a total cemented length of 300 *m* (984 *ft*). The steel modulus of elasticity is taken to be *200 GPa* and its Poisson ratio is taken as *0.3* so the steel shear modulus would be *76.9 GPa*.

When the Tree/BOP load is added to the casing system the assumption is that the upper casing is supported by tertiary layers of sand and layers of clay sediments as an elastic foundation and that the bottom of the lower casing supported by cement is also an elastic foundation. Hopefully, that combination will give a very small settlement at the mudline of less than 0.1 *m*. Here, using a mudline foundation modulus that is 1,000 times lower still would not yield large settlements. Therefore, even under the worst conditions the settlement at the Tree/BOP is less than the initial offset height of 3 *m* above the mudline. In other words, after any settlement, the Tree/BOP should still remain at least 2.5 *m* above the mudline after installation of the Tree/BOP.

Literature Survey

Biot (1937) introduced the effect of transverse elastic foundations on the deflections and stresses in beams. Hetenyi (1946) extensively extended such considerations in his classic book. Vesic (1963) extended the foundation model to have two parameters. Hetenyi and others have shown that settlement analysis based on the elastic foundation models can be an accurate, reliable method for determining structural displacements. Hetenyi mainly addresses the bending of beams and plates supported by transverse elastic foundations. He also gave several solutions for bars with axial elastic foundation supports. Hetenyi cites only a few values for the subsurface modulus. For deep rock layers he used a value of $k = 0.30\,GPa/m$ $(1{,}100\,psi/in)$. Kulhawy (1978) measured the foundation modulus for limestone as $k = 0.24\,GPa/m$ $(880\,psi/in.)$. NAVFAC (2011) lists the most recent values for sand and clay for marine applications. The US Army (2013) cites values for heavy load construction sites, and the California department of highways has guideline values for shallow soils which is now the ASTM standard D1883 – 14. Those values are tabulated in the Appendix.

The authors are unaware of any method to correlate the subgrade modulus to typical logging data such as shear wave velocities. Since the foundations respond through shear stresses it is likely that a correlation to shear wave velocities may exist.

The upper casing is similar to a deep pile, so the literature on piles was extensively reviewed. Most of the published works on axial elastic foundations deal with piles and shallow foundations of structures in civil engineering and repeat the derivation of Hetenyi (1946) (see Poulos and Davis (1990), Scott (1981) and Viggiani, *et al*. (2012)). Piles clearly are supported with elastic foundations. In the 1960's a number of field and laboratory tests were conducted and compared to analytic predictions. The results were reported in terms of the length to diameter ratio. Those data are of limited use since they did not include the *k* and *E* values needed for accurate displacement and stress determinations. For a circular pile the theoretical non-dimensional length governing the axial displacement is the Hetenyi constant *mL*. For a solid circular cross-section it simplifies to

$$m^2L^2 = [(PL)k]/[\,EA/L] = 4k(\pi D)L^2/E(\pi D^2) = 4kL^2/ED. \quad \ldots\ldots\ldots\ldots\ldots\ldots\ldots\ldots\ldots\ldots (1)$$

Thus, for constant physical moduli the behavior of a circular solid pile settlement and stress distribution is theoretically governed by the geometric parameter $L/\sqrt{D}$ instead of the non-dimensional ratio of L/D that is used in of most of the analytic and experimental studies of solid piles. However, the axial equilibrium solution (below) shows that the prior publications on piles should have reported the *mL* values and not the *L/D* values. Thus, those pile studies cannot provide useful insight into the current casing structural study.

The casing system equilibrium formulation presented in the next section gives the axial displacements and axial force in each casing segment. Since large axial compression forces were expected they should be compared to analytic equations for known buckling cases as a secondary safety check. Any buckling mode could significantly affect the seabed level settlements that are the main focus of this study. Therefore, literature on Euler and helical buckling were reviewed. The Euler buckling modes for slender members like piles are well known, see Craig (2000). Each higher Euler buckling mode reduces the effective column length, raises the buckling load, and increases by one the number of points where the casing would touch the open hole wall and thereby would increase the settlement at the seabed. For the *j-th* planar buckling mode the

critical Euler value is $F_{crit} = 4j^2\pi^2\, EI/L^2, n \geq 1$. If that critical load value is equated to the sum of the total Tree/BOP and member weights; and if the buckling length is taken as the total open hole length, then the mode number is approximately *j =24* and the casing would in theory deflect to the open hole wall 25 times. That makes a planar buckling condition unlikely to occur.

Considering any elastic foundation transverse support will change the planar buckling estimates since the Euler theory does not include that stabilizing effect. Also, support from a good cement job reduces the effective length and changes the transverse boundary conditions at the ends of the effective length. Hetenyi derived the higher planar buckling load for the condition where the beam is fully encased in a transverse elastic foundation. The stabilizing effect of the foundation produces a greatly increased *j-th* planar buckling critical load of $F_{crit} = 4j^2\pi^2\, EI/L^2 + 2\sqrt{DkEI}$ (see Hetenyi Chapter VII, page 148). That huge value essentially eliminates the possibility of planar Euler buckling when the casing is fully encased in cement. Thus, the free lengths and largest axial load from the current model should be compared to known helical buckling solutions. The literature on helical buckling was reviewed. Lubinski, *et al.* (1962) considered the settlement (total length change) for a weightless drill string that undergoes helical buckling. Later, Kwon (1988) extended that study by including the member weight. Kwon solved the fourth-order nonlinear differential equation for the post-buckled elastic equilibrium geometry and the total change in length in the string. The Kwon helical post-buckling solution was selected for use in this study. The Kwon solution includes the (unknown) diameter of the open hole. Here, it was assumed that the hole diameter is 101 mm (4 in.) larger than the OD of the lower casing. With that assumption it was determined that helical buckling would not occur for the system under study.

Governing Equilibrium Differential Equation with an Axial Elastic Foundation

The theoretical mechanics of this class of problem has been well established. The classic 1946 Hetenyi book on "Beams on Elastic Foundations" developed the (isothermal) governing differential equations for beams, shafts and bars embedded in an elastic foundation and subjected to bending, torsion, and axial loads. Making the assumption of constant foundation properties, he derived several analytic solutions, typically in the form of hyperbolic sine and cosine functions. His theoretical solutions compare well with experiments and numerical simulations. The same governing equations and solutions are given by (Scott, 1981) and by (Viggiani*, et al.* 2012). In theory, Hetenyi's solutions could be extended to foundations of layers with different properties, but published solutions have been limited to foundations with two layers. Here, the top tertiary layers of sand and layers of clay sediments provide axial foundation support for the upper casing. The large middle segment of the lower casing length is surrounded by open hole. The layer of cement at the lower region of the smaller casing also provides foundation support.

The governing one-dimensional equation of equilibrium for the settlement, *u(z),* of an axisymmetric casing embedded in an axisymmetric axial foundation is:

$$\frac{d}{dz}\left[E(z)A(z)\frac{du(z)}{dz} - EA\alpha(z)\Delta T(z)\right] + P(z)k(x)[u(z) - u_\infty] + \mathrm{w(z)} = 0, \quad \ldots\ldots\ldots\ldots\ldots\ldots (2)$$

where all the data can vary with the vertical location, *z*. Those data are: u_∞= a known settlement (almost always zero) measured at location considered to be at infinity [L], *E* = casing elastic modulus [F/L^2], α = casing coefficient of thermal expansion [L/L K], γ = casing weight per unit volume [F/L^3], *A* = cross-sectional area of the casing [L^2], *P* = outer perimeter of the casing [L], *k* = the foundation modulus of the lithology [F/L^2/L], *w* = the vertical line load on the casing, usually $w = \gamma A$ [F/L], ΔT = the temperature increase from the stress free state [K]. Point forces [F] are a special case of the axial line load *w(z)* and can also be applied at any point along the casing. The top point load will come from the Tree weighing approximately *747e3 N* (*168e3 lb*) and BOP weighing approximately *4.45e6 N* (*1e6 lb*). Of this, the rig tensioners are assumed to support *2.22e6 N (500e3 lb)* giving a net downward weight on the well head of approximately *2.971e6 N (668e3 lb)*. For the

Angola casing, the bottom of the lower casing section is initially free before the cement is installed; so the linear temperature change with depth will create a small change in length but no axial stress. Thus, the temperature data were omitted here.

Unlike most structural studies, the casing does not usually have one or more points of specified settlement, which is usually an essential boundary condition for a second order differential equation. Instead, the clastic layers of sand and layers of clay sediments and the cement foundation moduli *k(z)* provide the necessary vertical support to prevent the rigid body motion. A typical solution for the settlement displacement involves the hyperbolic cosine, such as $u(z) = c_1 + c_2 \cosh[m(L-z)] / \cosh[mL]$ where the positive constant is $m^2 = Pk/EA$. Note that the parameter governing the rate of change of the axial displacements is the non-dimensional length parameter $n = mL$. Here, this has a physical interpretation since

$$n^2 = m^2 L^2 = \frac{(PL)k}{EA/L} \quad \ldots\ldots (3)$$

is the ratio of the total foundation stiffness to the casing axial stiffness. The constant *m* has the units of [1/L]. The analytic solution for the stress in the casing, $\sigma = E\varepsilon = E\ du/dz$, in a region with an elastic foundation is in the form of a hyperbolic sine function: $\sigma(z) = Ec_2 \sinh[m(L-z)] / \mathrm{m} \cosh[mL]$. In theory, systems with layered constant properties can be formed by combining such solutions. For this partially open hole case, the upper and bottom section settlements will have a cosh variation of axial displacements while the open hole segment will have a quadratic displacement variation with depth. Since the data for the current casing study are spatially varying and often discontinuous, an equivalent finite element integral form is used here to obtain a numerical solution as given by (Akin, 2005) and others. An element interface is placed at any *z* location where a discontinuity occurs for any of the above data. That sets the minimum mesh that can be used for the actual casing analysis.

Classic Axial Member Equilibrium Equation

It is the presence of the coupling foundation modulus, *k*, which significantly changes the nature of the spatial solution from that of the classic axial loading of a bar. When *k = 0,* in an open hole region, the above equation of equilibrium reduces to the one for the classic axial bar displacement, *u(z)*:

$$\frac{d}{dz}\left[E(z)A(z)\frac{du(z)}{dz} - EA\alpha(z)\Delta T(z)\right] + \mathrm{w(z)} = 0. \quad \ldots\ldots (4)$$

This can simply be integrated twice, along with the appropriate boundary conditions to obtain a solution. Then, for the isothermal case and a constant load per unit length, $w = W/L$, the displacement has a quadratic variation with the axial position and the axial stress varies linearly with the position. The most common example is a casing simply hanging from its top support. There the axial stress varies from zero at the bottom linearly to a maximum value of $\sigma_{max} = \mathrm{W/A} = \gamma\mathrm{AL/A}$ while the displacement increases quadratically from zero at the top to a maximum at the bottom of $u_{max} = WL/2EA$. At the midpoint the axial stress is half the maximum and the displacement is 3/4 of the maximum. Conversely, if the top is free and the bottom is fixed the values reverse locations and signs.

Cubic Axial Bar and Foundation Finite Elements

The general differential equation (1) for an axial member embedded in an elastic foundation was converted to an equivalent integral (work energy) formulation and implemented as a one-dimensional finite element model. Due to the spatial nature of the analytic solution, cubic finite element line members were used instead of the common linear or quadratic line elements used for simple bars and shafts. The cubic elements are assembled into a matrix equilibrium system. After enforcing any known displacements, that system is solved for the settlement displacement along all casing members. If known displacements are prescribed, then the corresponding reaction force is recovered after all the displacements have been calculated.

Without the foundation, the exact axial deflection and stress in an isothermal casing can be obtained with a quadratic displacement (three-node) line element, even for layered data. Cubic line elements have been tested against analytic solutions for the axial member in an elastic foundation and they yielded a maximum error of less that 0.1% when a reasonable mesh is used. The cubic displacement element has four nodes equally spaced along the length of the element. Within each element the axial displacement is interpolated as

$$u(x) = u_1^e(1 - r\,11/2 + 9r^2 - 9r^3/2) + u_2^e(9r - 45r^2/2 + 27r^3/2) + u_3^e(-9r/2 + 18r^2 - 27r^3/2) + u_4^e(r - 9r^2/2 + 9r^3/2), \quad \text{(5)}$$

where u_j^e is the displacement at the j-th node of element number e, and $r = z/L^e$ is the non-dimensional length along the element. If a foundation is present along the length of the element then the cubic polynomial is a piecewise approximation of the actual cosh (z) displacements along the element. If no foundation is present along the length of the element, then the computed displacements combine to reduce this to the exact quadratic displacement of a hanging bar, with or without external axial forces.

Using this displacement interpolation the stress, $\sigma = E\varepsilon = E\ du/dz$, is approximated along the element as

$$\sigma = E\varepsilon = E\ du/dz = E[\,u_1^e(-11/2 + 18r - 27r^2/2) + u_2^e(9 - 45r + 81r^2/2) + u_3^e(-9/2 + 36r - 81r^2/2) + u_4^e(1 - 9r + 27r^2/2)]\,/\,L^e\,. \quad \text{(6)}$$

If no foundation is present along the length of the element, then the computed displacements combine to reduce this to the exact linear axial stress of a hanging bar, with or without external axial forces. If a foundation is present along the length of the element then the quadratic polynomial is a piecewise approximation of the actual sinh (z) axial stress along the element. In the cubic polynomial case, there is a small discontinuity in the stress at each element interface. When a proper mesh is employed the jump in stress is so small that it cannot be seen in a force versus position graph. The axial casing force at any location is found by multiplying the axial stress at any point by the cross-sectional area, $\mathrm{F} = \mathrm{A}\,\sigma$. For the upper casing, one cubic element was above the mudline and five were below the mudline. The lower casing had 17 cubic elements, giving a total of 22 elements and 67 displacement nodes. Their lengths were varied, based on experience, to be smaller in regions where rapid changes were expected.

The axial stiffness matrix for each cubic bar element is

$$\boldsymbol{K_E}^{\boldsymbol{e}} = \frac{E^e A^e}{40 L^e}\begin{bmatrix} 148 & -189 & 54 & -13 \\ -189 & 432 & -297 & 54 \\ 54 & -297 & 432 & -189 \\ -13 & 54 & -189 & 148 \end{bmatrix} \quad \text{(7)}$$

and the additional stiffness matrix for an element having the elastic foundation along its length is

$$\boldsymbol{K_F}^{\boldsymbol{e}} = \frac{k^e P^e L^e}{1680}\begin{bmatrix} 128 & 99 & -36 & 19 \\ 99 & 648 & -81 & -36 \\ -36 & -81 & 648 & 99 \\ 19 & -36 & 99 & 128 \end{bmatrix}. \quad \text{(8)}$$

The foundation stiffness is directly proportional to the surface area, $P^e L^e$, of its contact with the casing element. If the element's net casing weight per unit length is constant its resultant force vector is

$$\boldsymbol{F_w}^{\boldsymbol{e}} = \frac{w^e L^e}{8}\begin{Bmatrix} 1 \\ 3 \\ 3 \\ 1 \end{Bmatrix}. \quad \text{(9)}$$

When all of the elements are assembled the system matrix equation of equilibrium, including external point loads, say $\boldsymbol{F_z}$, is

$$[\boldsymbol{K_E} + \boldsymbol{K_F}]\{\boldsymbol{u}\} = \{\boldsymbol{F_w}\} + \{\boldsymbol{F_z}\}. \quad \text{(10)}$$

Inverting the combined stiffness matrix yields the axial displacements of all nodes in the system, $\{\boldsymbol{u}\}$, and thus the displacements of each element, $\boldsymbol{u^e}$. The element displacements yield the axial stress and axial force at any location in the casing string and are plotted along its length. The load transferred from a casing segment to the elastic foundation element is also available. In a foundation element the force per unit length at each of the four nodes is $\boldsymbol{f^e} = \boldsymbol{K_F}^{\boldsymbol{e}}\, \boldsymbol{u^e}$. That load per unit length is integrated along each element to obtain the total force on the casing coming from that element. Those data are accumulated to give the total axial force on the casing from the foundation along the length of the casing. The sum of the axial reaction forces (if any) and the total axial foundation force (if any) is equal and opposite to the total applied load from the member weights and any external axial point (Tree/BOP) load. All of those values are listed as output from the finite element calculations. In addition, the settlement displacement, casing axial stress, and foundation axial loads on the casing are plotted as a function of depth.

Casing Foundation Settlement in Four Incremental Loadings Stages and Their Combination

To understand if large settlement or helical buckling needs to be a concern at the Cameia development in Angola one should understand the stresses and forces that develop in each phase of its construction and the final state resulting from their combination. Below the results for 1: installing the upper casing, 2: hanging the lower casing from the upper casing, 3: adding cured cement to lower portion of the smaller casing, and 4: adding the Tree/BOP to the top of the casing system; are given for the casings and foundations.

1: Upper Casing Installation

First, the upper casing was jetted into the clay sediments to a depth of approximately 99 *m*, with approximately 3 *m* remaining above the mudline. The top foundation consists of layers of sand and layers of clay sediments. A relatively low foundation modulus of 40.7e6 $N/m^2/m$ (150 $lb./in^2/in$) was assumed for that region. The upper casing and the foundation deforms under just the weight of the upper casing. Of course, the entire upper casing settles into the upper foundation region. The settlement at the mudline due just to that weight was very low, approximately 8.6e-5 *m*, and rapidly drops to approximately 6.9e-5 *m* at the bottom of the casing. The settlement shape (axial displacement) is in **Fig. 2**.

The axial forces in the upper casing are in **Fig. 3**, which shows almost a step change from zero up to a maximum of approximately -2.4e4 *N*. The reaction force from the foundation applied to the upper casing is in **Fig. 4** and increases linearly with depth from zero at the mud line to the weight of the upper casing (approximately 8.24e5 *N*) at the bottom. The gradient of the foundation force can be used to approximate the shear stress in the sediments. The approximate axial distribution of the upper foundation shear stress is given in **Fig. 5**. There is nearly a step change up to a maximum of approximately 3.4e3 which drops rapidly to a minimum of 2.8e3 N/m^2. The maximum shear stress in this case is only 16 % higher that the uniform value computed as the upper casing weight divided by its surface area in contact with the sediments. These quantities are all quite small compared to the same quantities in the final load state.

2: Hanging the lower casing

At the end of the first stage of construction the entire lower casing and its shoe are hung from the upper casing approximately 3 m above the mudline. That places additional compression on the upper casing and causes additional settlement of the clastic sediments foundation. The lower casing hangs from its top and is partially supported by buoyancy force on the shoe. The net upward force on the shoe is $F_S = 1.763e6\ N$ $(3.964e5\ lb)$. The settlement shape, before the cement job, of the upper casing and lower hanging casing is in **Fig. 6**. As expected, the lower casing axial displacement is that of the classic hanging bar loaded at its bottom. The mudline settlement from this load cases is approximately 0.0017 *m*, assuming a foundation modulus of 40.7e6 $N/m^2/m$ (150 $lb./in^2/in$).

The axial force distribution appears in **Fig. 7**. The axial compression force on the upper casing drops rapidly from a maximum compression of approximately -2.13e6 *N* at the mudline to near zero at the top of the open hole. The lower casing axial force has maximum tension at its top and drops linearly to the upward compressive shoe force at the bottom ($-1.763e6\ N$). That force graph shows that the initial *neutral point* for the lower casing is at approximately the 685 m point (approximately 501 m above the shoe).

The casings stresses have a similar distribution as the axial forces since their two respective areas are constant. The reaction forces from the foundation acting on the upper casing are in **Fig. 8**. It increases rapidly from zero and then reaches a maximum of approximately 3.0e6 *N*. The foundation forces act only on the sediments foundation at the top of the upper casing, at this stage. The system remains in that state until the cement cures at the bottom of the hole and the Tree/BOP are added.

The approximate shear stresses in the upper sediments are given in **Fig. 9**. There is an approximate step change to the maximum shear stress (at the mudline) of approximately 5.1e4 N/m^2 and it rapidly drops off to approximately 0.3 N/m^2. The peak value is approximately five times higher than a simple constant value estimate based on the exterior surface area, below the mud line and the upper casing weight.

3: Adding the Tree/BOP with no cement

To better illustrate the effect of good and poor cement on this system the addition of the Tree/BOP to the above case, where no cement is present, will be considered next. Since there are not yet any displacement supports at the bottom of the lower casing the entire additional Tree/BOP load (2.971e6 *N*) would be carried just by the upper sediment foundation. Thus, the upper casing displacements increase, from approximately 1.7e-3 to 4.1e-3 *m* at the mudline, as shown in the zoomed in view of **Fig. 10**. The general shape and magnitude of the lower casing displacements remain as basically shown in Fig. 6. A zoomed in view of the increased axial force in the upper casing is shown in **Fig. 11** (to contrast with Fig. 7). The axial forces in the upper casing and sediments would increase by approximately a factor of 2.4 to approximately -5.1e6 *N*, without cemented support. The corresponding forces from the upper sediments are shown in the zoomed view of **Fig. 12** (compare to Fig. 8). Likewise, the approximate shear stress distribution is given **Fig. 13** (compare to Fig. 9).

4: Setting of the cement

In this numerical simulation the setting of the cement simply means setting a non-zero cement subgrade modulus to replace the prior zero value used before the cement cured. None of the displacements or stresses change since the concrete simply went from fluid to solid. However, the next loading of applying the Tree/BOP will then also be resisted by the cement section.

5: Adding the Tree/BOP to a cemented string

Next, the effects of the cement job were considered in resisting the Tree/BOP loading. After setting, cement will serve as a second elastic support for the casing when it is subjected to any future load state. When the Tree/BOP are subsequently added to the top of the upper casing that load will be supported jointly by the top clastic sediment foundation and the cement acting along some height of the lower casing. That load state causes an increment in the deflection, stresses and forces that add to the prior case of the hanging lower casing subject to the shoe buoyance force. In this incremental study, the casing weights and the upward shoe force are omitted (since they was used in the hanging load state above), the weight of the Tree/BOP is added to the top of the upper casing, and the cement is assumed to provide distal support to the lower casing with a cement foundation modulus of 81.4e6 $N/m^2/m$ (300 $lb./in^2/in$), and a cured height of 300 *m*. The bottom node was fixed. (Note that the height of the cement, and/or its foundation modulus is easily modified as input data.) For this load state, the incremental settlement shape is shown in **Fig. 14**.

A zoomed in view of the incremental forces in the upper casing region is given in **Fig. 15**. In that region, and until the cement line is reached, the lower casing has a constant incremental compression of approximately -2.2e4 *N*. The incremental compression of the upper casing drops from approximately -3.0e6 *N* to zero at its bottom. Not shown is that the much smaller incremental compression in the lower casing drops to essentially zero approximately 35 *m* below where the casing enters the cement at 900 *m*.

The original goal of this study was to predict the mudline settlement when the Tree/BOP is added. Adding the above mudline displacement to the value before placement of the Tree/BOP predicts a very small total settlement of approximately 0.0064 m. The main interest is how much of the total set of loads is split between the upper sediment foundation and the cement foundation. The upper region of the lower casing is in tension after the cement sets. Therefore, the upper sediments will tend to support most of the incremental loading. How much depends on the sediment modulus compared to the cement modulus. For very weak sediments the cement absorbs most of the Tree/BOP weight, but the load distribution reverses for strong sediments. This is illustrated by considering the variation of the forces and corresponding shear stresses as the sediment modulus is reduced and the cement modulus is held at a high quality value.

Effect of foundation moduli

In this study the two major assumed physical variables are the sediment foundation modulus, say k_s, of the sediments adjacent to the upper casing, and the quality of the cured cement adjacent to the lower casing herein represented by its foundation modulus, say k_c. Here, the length of the upper and lower foundations and the length of the intermediate casing in between and the other physical data are based on those from a single well. A simplification of this model, at the time that the Tree/BOP is installed, is that it is primarily a series of springs consisting of the mudline spring, the intermediate casing spring, and a bottom cement spring. Here, the intermediate casing between the two foundation springs is so long that its stiffness (*EA/L*) is relatively low. That means that in the current study, where all of the assumed lengths are held constant, k_s is the main factor in determining how the additional Tree/BOP load is split between the upper sediments and the bottom cement. The elastic foundation lengths are quite important and the final load sharing is actually governed by the relative non-dimensional stiffnesses of the foundation regions compared to the casing axial stiffness: $n^2 = [(PL)k]/[EA/L]$. The current software is capable of varying the location, length, and modulus of any axial elastic foundation. Here, only a few values of k_s have been investigated to evaluate the sharing of final the Tree/BOP load. Those results are given in **Table 1**.

Table 1 Percent of BOP/Tree Incremental Load Carried by Elastic Foundations**

k_s / k_c	1/2	1/10	1/100	1/1,000	1/10,000
Sediment %	99	98	96	70	20
Cement %	1	2	4	30	80
n_s^2/n_c^2 *	0.03979	0.007958	0.000796	0.000080	0.000008

* Based upon specific lengths given above

** For fixed intermediate casing stiffness

The actual physical foundation modulus of the tertiary layers of sand and layers of clay provide a large portion of the support of the Tree/BOP. However, currently that modulus clearly is impractical to measure and it has not yet been correlated to acceptable logging data. It will not be zero, but jetting procedures are known to leave gaps around the outside of the upper casing that could render the effective modulus insufficient. Finding a way to estimate that modulus would make this theoretical study more useful.

It is clear that another set of important variables, for sharing the Tree/BOP incremental load, is the length of the cemented region, say L_c, and the quality of the cement. Increasing L_c reduces the unsupported length of the inner casing thereby inversely increasing its axial stiffness. But, even cementing the full casing length is of no use if the cement is of very poor quality ($k_c \Longrightarrow 0$). To address the continuing question of how long the cemented region needs to be requires a future parametric study where the cemented region, L_c, and its quality, k_c and/or n_c^2, are varied over practical ranges.

Conclusions

Settlement analysis based on the elastic foundation model provides a theoretical method for determining the axial displacements. The assumption that the upper casing is supported by tertiary layers of sand and layers of clay sediments that form an elastic foundation and that the bottom of the lower casing is supported by cement treated as an elastic foundation gives a very small settlement at the mudline, when the Tree/BOP are added.

Here, even using a foundation modulus that is 1,000 times lower than the initially assumed value still would not yield large settlements. Therefore, even under the worst mudline conditions the settlement is less than the initial offset height of 3 *m* above the mudline. In other words, the current data predict that the Tree/BOP should still remain at least 2.5 *m* above the mudline after the installation of the Tree/BOP. This type of analysis was applied to one well in Angola Cameia. The actual settlement could not be measured but video footage from an ROV confirmed that it was too small to observe.

The detailed analysis of the casing embedded in an elastic foundation, assuming a structurally active top clastic sediment region, leads to the conclusion that (for the length of cement considered) the lower casing cement only supports a significant portion of the Tree/BOP when the clay sediment foundation is very weak. Finally, note that if the cement job were to have undesirable gap regions that could be identified by logging measurements then those disjointed foundation support regions could easily be included in this type of finite element settlement analysis.

Acknowledgements

This study was supported by Cobalt International Energy Incorporated of Houston, TX.

Notation

A = cross-sectional area of the casing, m^2

α = casing coefficient of thermal expansion, m/m°C

E = casing elastic modulus, N/m^2

ε = axial strain, m/m

F_{crit} = magnitude of an axial buckling force, *N*

$\boldsymbol{F_w^e}$ = resultant axial weight force on casing element, *N*

$\boldsymbol{F_z}$ = system matrix of known point forces, *N*

γ = casing weight per unit volume, N/m^3

k = the foundation modulus of the lithology or cement, *MN/m²/m*

k_c = foundation modulus of the bottom cured cement, *MN/m²/m*

k_s = foundation modulus of the upper sediments, *MN/m²/m*

$\boldsymbol{K}$ = assembled stiffness matrix of all casing and foundation elements, N/m

$\boldsymbol{K_E^e}$ = axial stiffness matrix of the casing element, N/m

$\boldsymbol{K_F^e}$ = axial stiffness matrix of the surrounding foundation element, N/m

L = length, *m*

L_c = length (height) of concrete around bottom casing, *m*

n^2 = ratio of the foundation stiffness (P L k) to the casing axial stiffness (EA/L)

P = outer perimeter of the casing, *m*

ΔT = the temperature increase from the stress free state, °C

u_∞ = a known settlement measured at location considered to be at infinity, *m*

$\boldsymbol{u^e}$ = matrix of displacements at nodes of a casing element, *m*

$\boldsymbol{u}$ = matrix of displacements at all casing nodes, *m*

w = the vertical line load on the casing, usually $w = \gamma A$, N/m

W = total weight of a casing, *N*

z = axial position, *m*

References

Akin, J.E. 2005. *Finite Element Analysis with Error Estimators*, London: Elsevier.

Anderson, K.A. 1984. "Support Systems For High Wellhead Loads", *Journal of Canadian Petroleum Technology,* 12(3):76-78.

ASTM, 2014. Standard Test Method for California Bearing Ratio (CBR) of Laboratory-Compacted Soils, D1883 – 14.

Biot, M.A. 1937. Bending of an Infinite Beam on an Elastic Foundation, *J. of Applied Physics*, 12(2): 155-164.

Craig, R.R. 2000. Chapter 10, *Mechanics of Materials*. New York: Wiley and Sons.

Duan, W.H., Wang, C.M. 2008. "Exact Solution for Buckling of Columns Including Self-Weight", Journal of Engineering Mechanics, 134, (1), 116-119.

Hetenyi, M., 1946. *Beams on Elastic Foundation*, Ann Arbor: University of Michigan Press.

Kulhawy, F.H. 1978. Geomechanical Model for Rock Foundation Settlement, J. *Geotech. Eng. Div., ASCE*, 104, 2, 211-227.

Kwon, Y.W.1988. "Analysis of helical buckling", SPE Drilling Engineering, 3, 21I-216.

Lubinski, A., Althouse, W.S. & Logan, J.L. 1962. "Helical Buckling of Tubing Sealed in Packers", J. Petro. Tech., 14, 665-670.

NAVFAC 2011., *Handbook for Marine Geotechnical Engineering*, SP-2209-OCN.

Poulos, H.G., & Davis, E. 1980. Pile Foundation Analysis and Design. New York: Wiley and Sons.

Randolph, M., & Wroth, C. 1978. "Analysis of Deformation of Vertically Loaded Piles", J. Geotech. Eng. Div., ASCE, 104, 12, 1465-1488.

Scott, R.F. 1981. *Foundation Analysis*, Englewood Cliffs: Prentice Hall.

US Army 2013. Concrete Floor Slabs on Grade Subjected to Heavy Loads, TM 5-809-12.

Vesic, A.B. 1963. "Beams on Elastic Sub-grade and the Winkler's Hypothesis". Proceedings, 5th Intern. Conference of Soil Mechanics, pp. 845-850.

Viggiani, C., Mandolini, A. and Russo, G. 2012. *Piles and Pile Foundations*, London: Spon Press.

Appendix: The Elastic Foundation Modulus

For concrete, the foundation modulus has been reported with values ranging from *28.8 MN/m^2/m* (*106 lb./in^2/in)* to *81.4 MN/m^3* (*300 lb./in^2/in*). Of course, test cylinders could be retained and tested using a modification of the above ASTM definition of its foundation modulus. **Tables 2, 3, and 4** give subgrade modulus values.

Table 2 Typical Modulus, k, (lb./in^2/in) for Shallow Foundations [US Army 2013]

Moisture content	1-4	5-8	9-12	13-16	17-20	21-24	25-28	>=29
Silts & Clays		200	175	150	125	100	75	50
Silts & Clays & Sand	300	250	225	200	150			
Large Sand	300+	300	250					
Silt & Clay & Gravel	300+	300+	300	250				
Gravel & Large Sand	300+	300+						

Table 3 California Bearing Ratio (CBR) Foundation Moduli Rankings [ASTM D1883–14]

Strength	CBR	k, lb./in^2/in	k, MN/m^2/m
High	15	550	149.3
Medium	10	300	81.4
Low	6	150	40.7

Ultra Low	3	75	20.4

Table 4 Average Subgrade Modulus for Soil Types [NAVFAC]

Description	k, lb./in^2/in	k, MN/m^2/m
Loose sand	8.84	2.40
Medium sand	19.0	5.15
Dense sand	28.6	7.75
Soft clay	22.1	6.00
Medium clay	39.6	10.8
Stiff clay	69.0	18.8
Very stiff clay	144.0	39.0

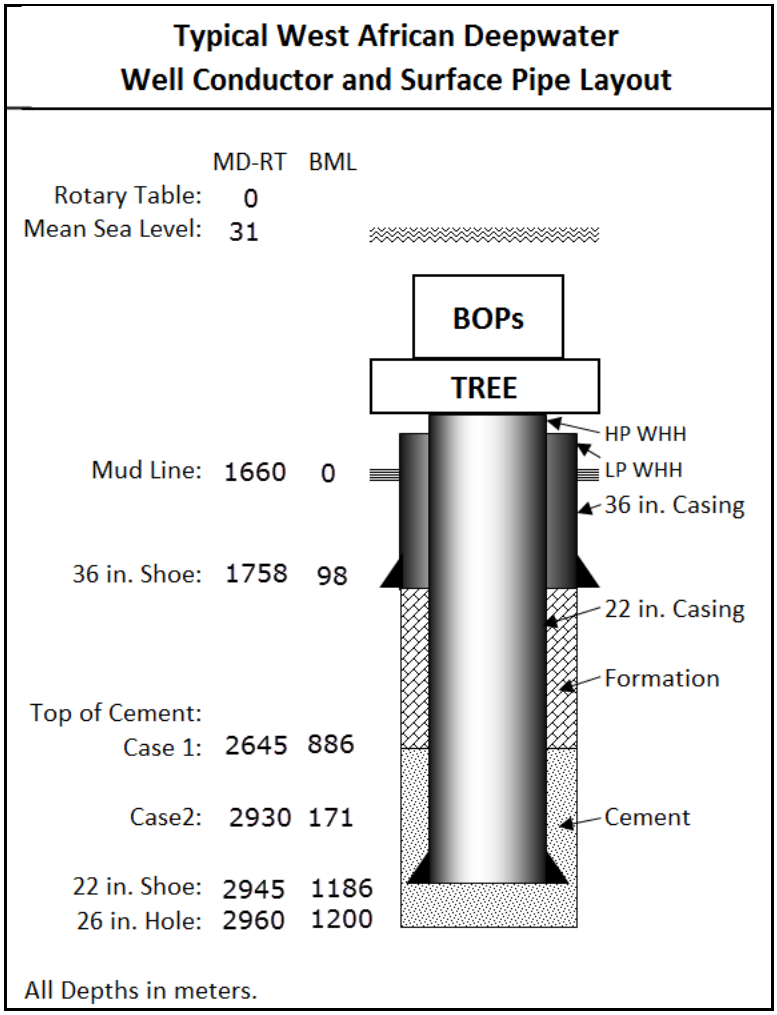

Fig. 1 Schematic of the casing system and axial foundation regions

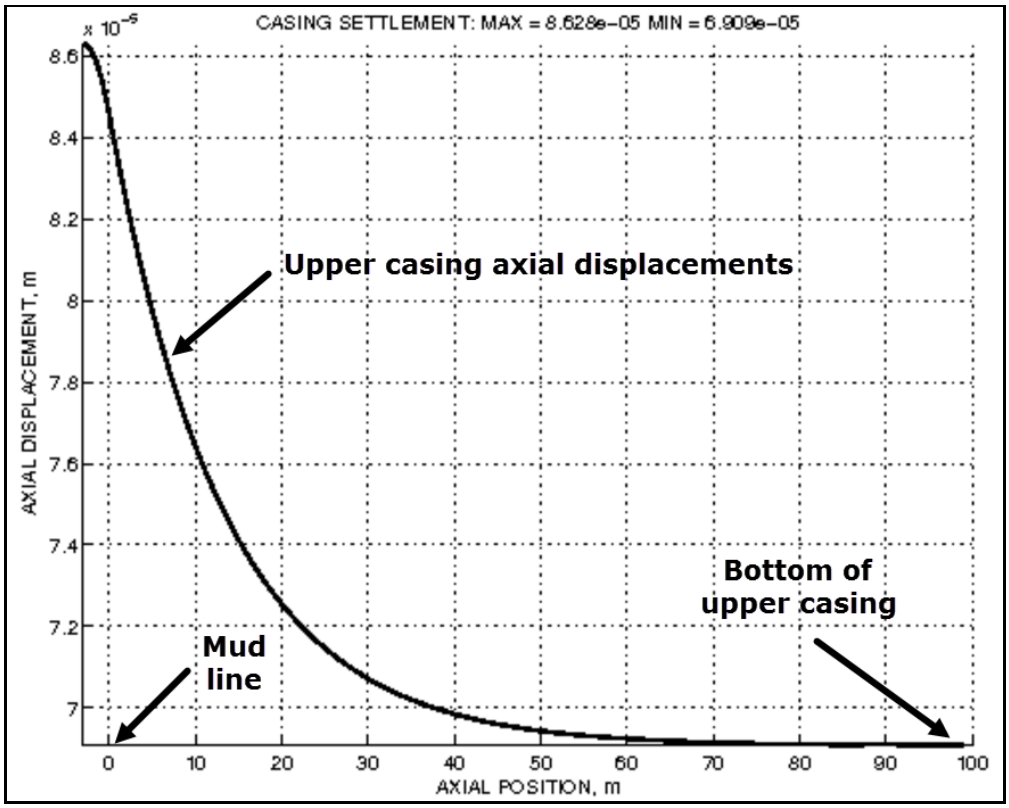

Fig. 2 Initial axial settlement of upper casing from self-weight

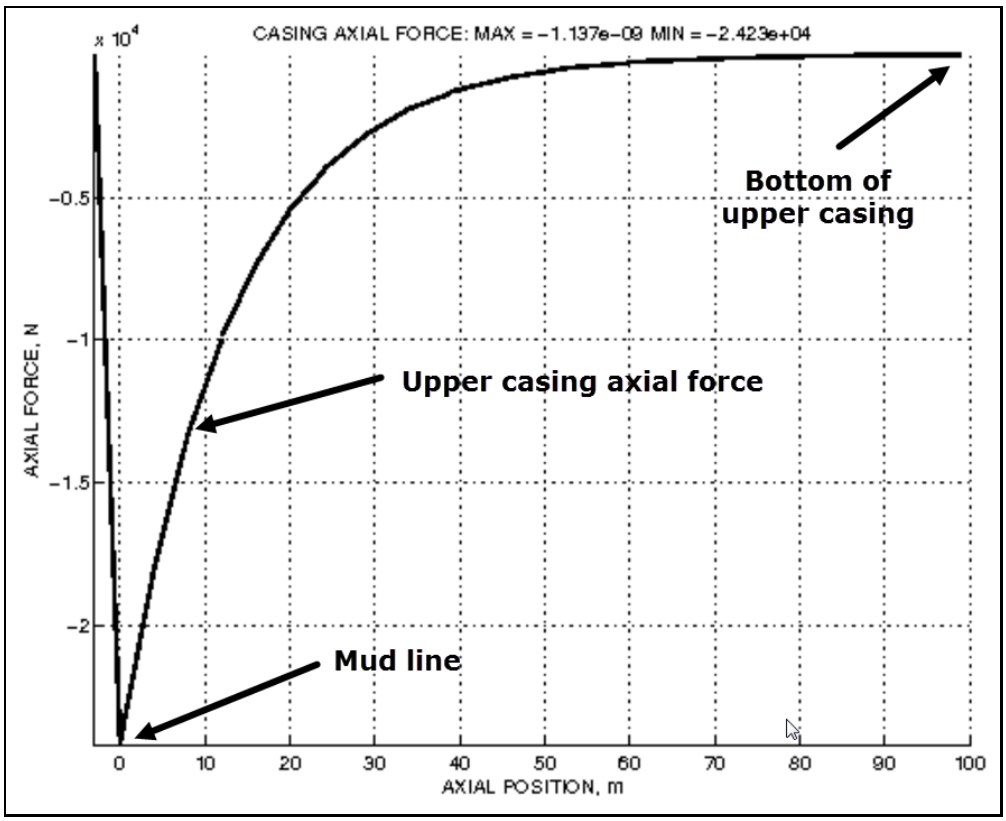

Fig. 3 Initial axial forces in upper casing from self-weight

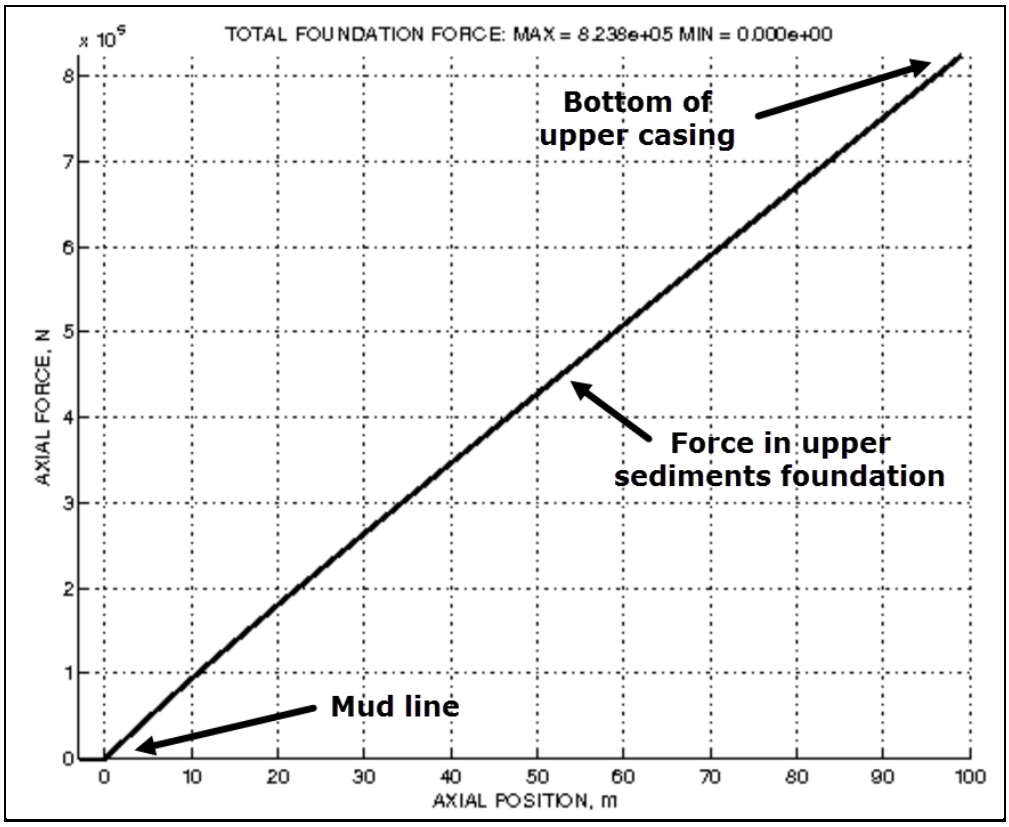

Fig. 4 Initial foundation forces on upper casing from upper casing

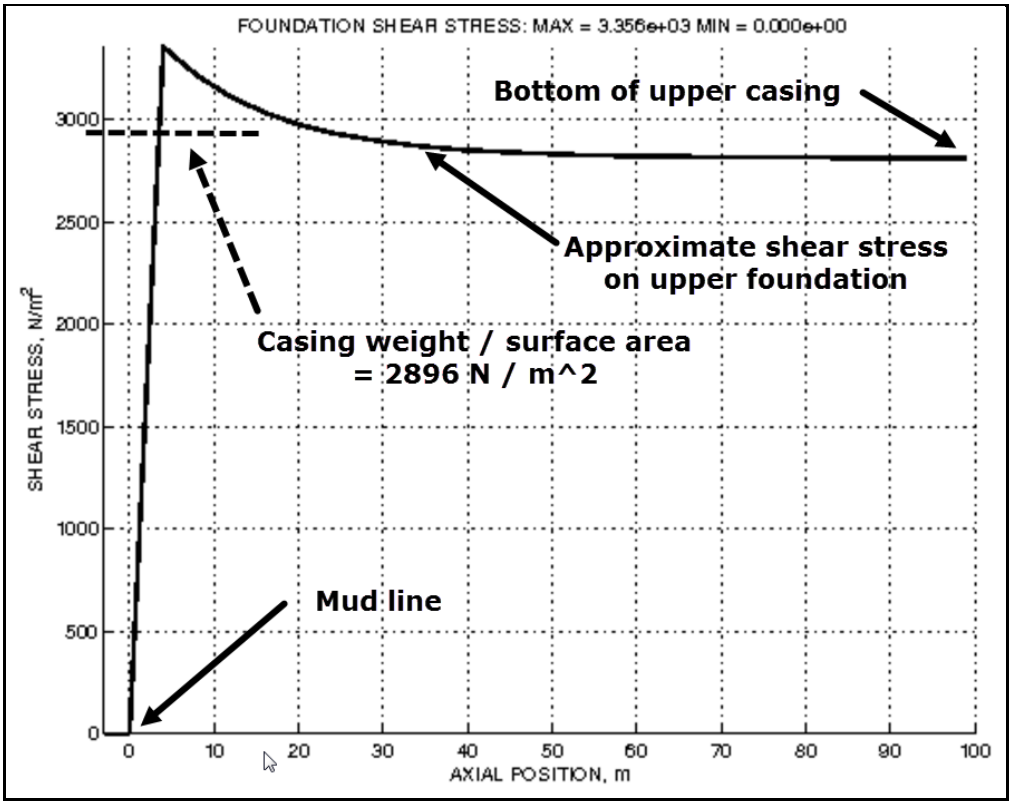

Fig. 5 Approximate shear stresses in upper sediments from upper casing weight

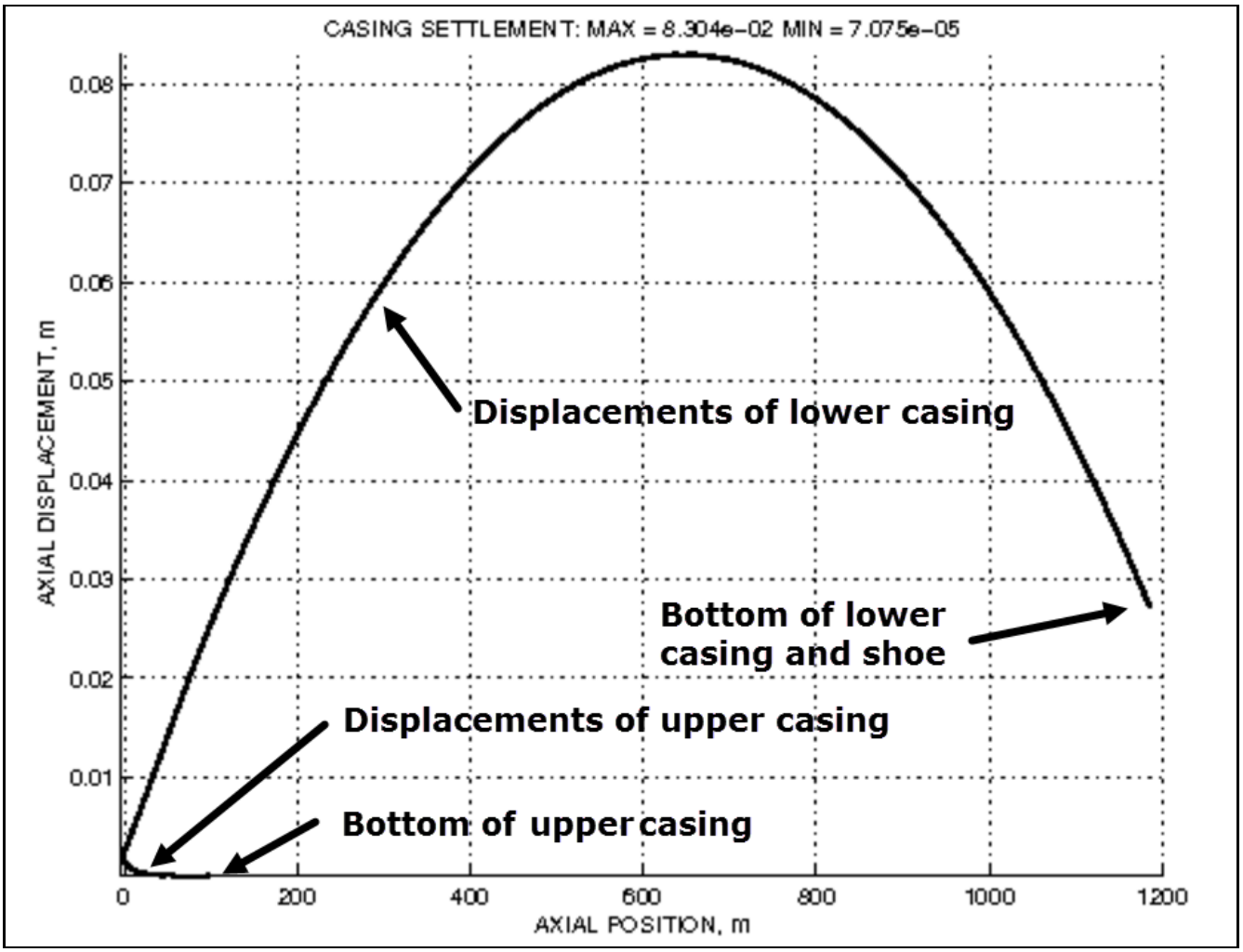

Fig. 6 Axial settlements from both casing weights and shoe force

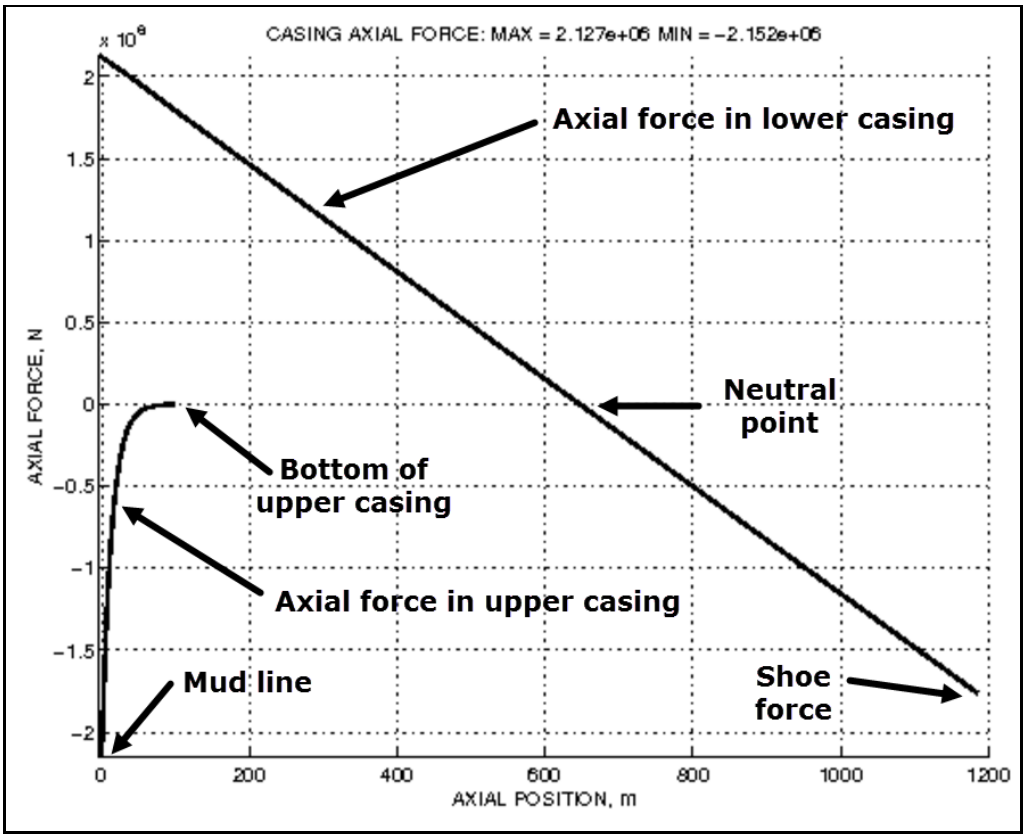

Fig. 7 Axial forces in the casings from casing weights and shoe force

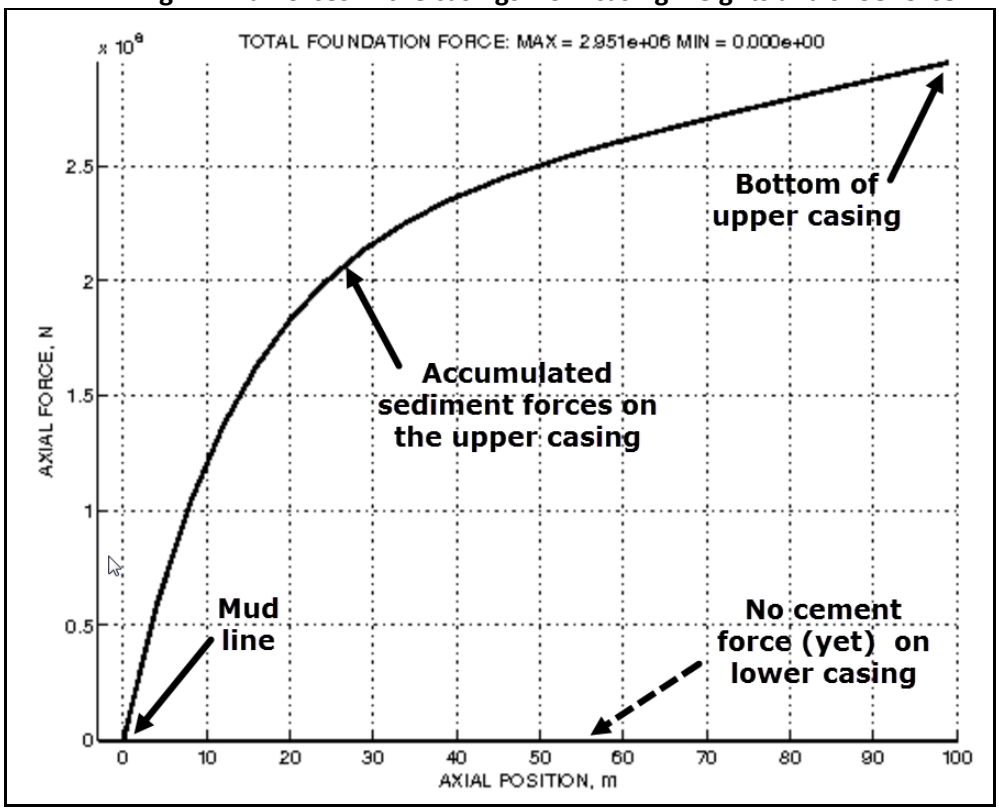

Fig. 8 Upper foundation axial forces (top) from both casing weights and shoe

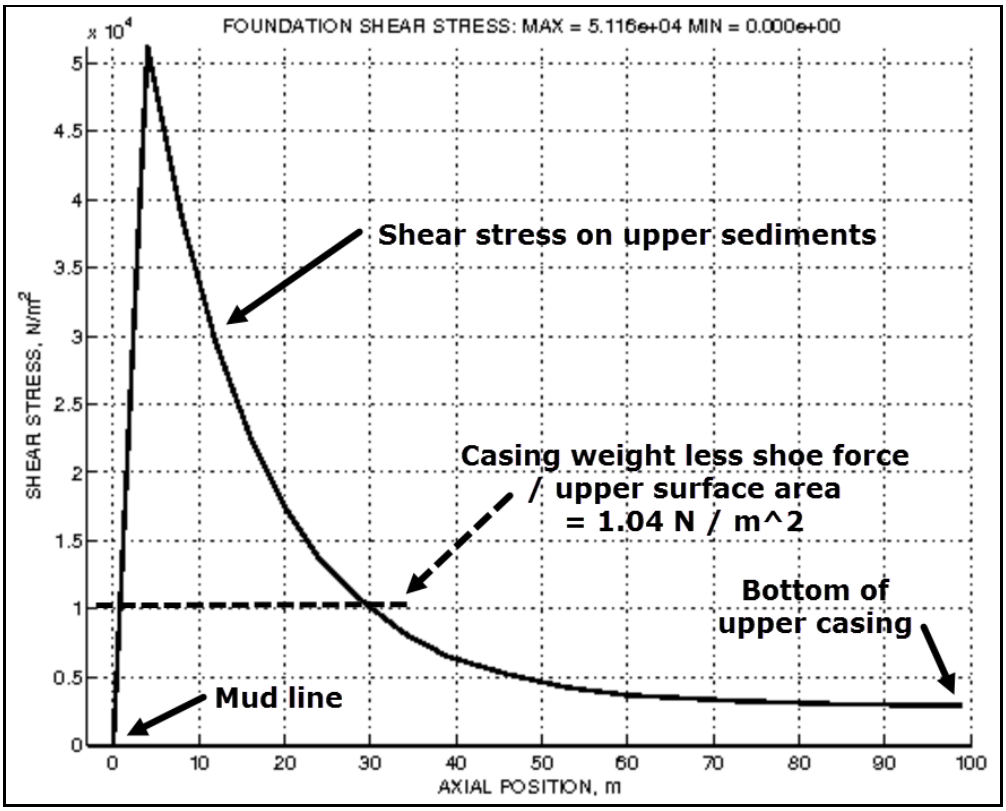

Fig. 9 Shear stresses in upper sediments (top) from both casing weights and shoe force

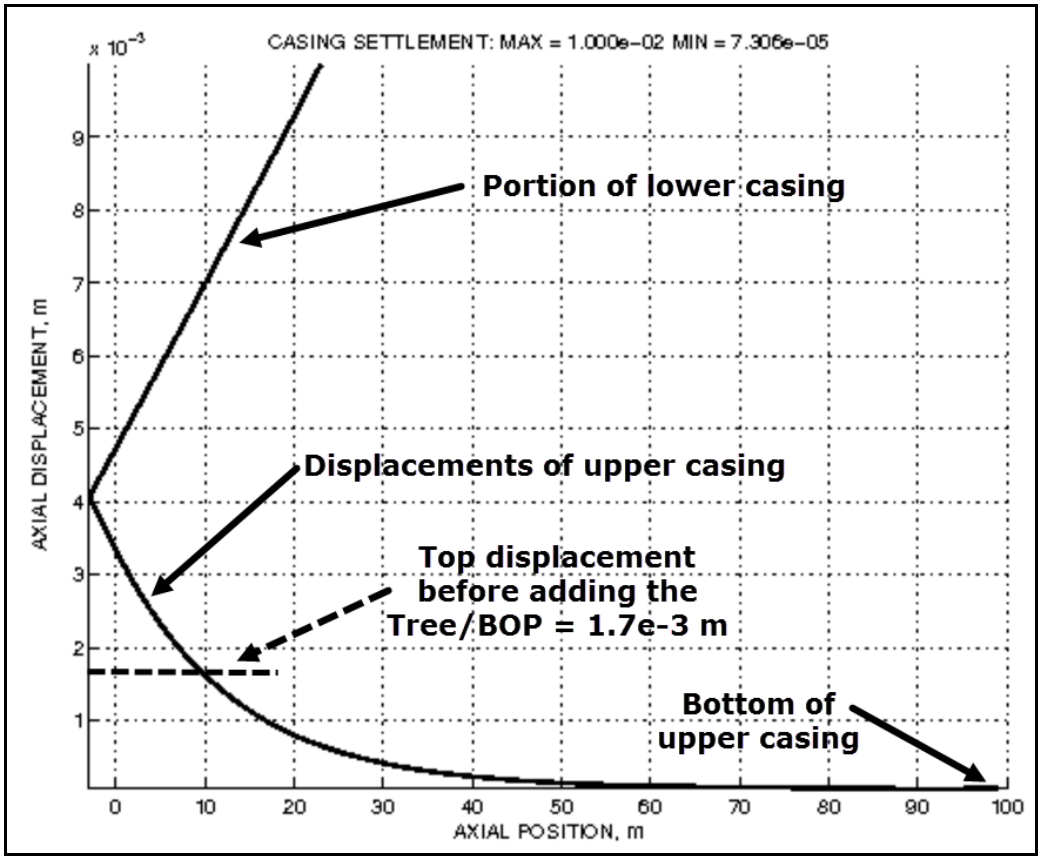

Fig. 10 Without cement, the upper sediments displacements increase from the Tree/BOP weight

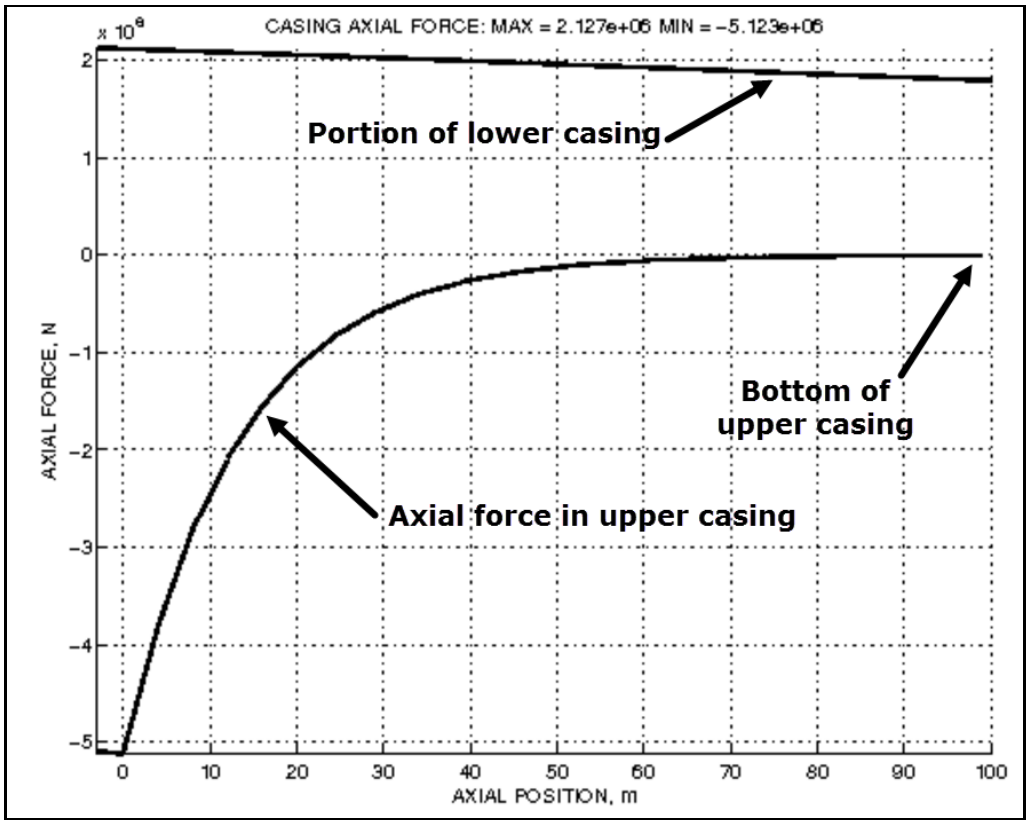

Fig. 11 Upper casing axial forces if Tree/BOP is added without cementing (bottom)

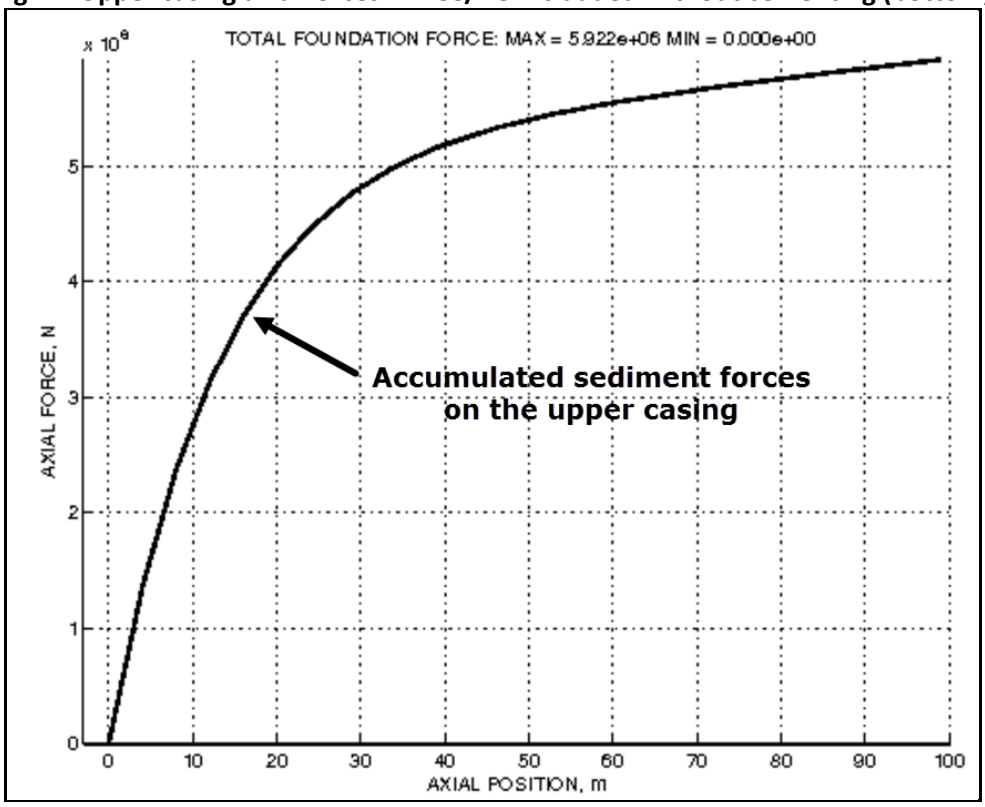

Fig. 12 Upper foundation axial forces, if Tree/BOP is added without cementing (top)

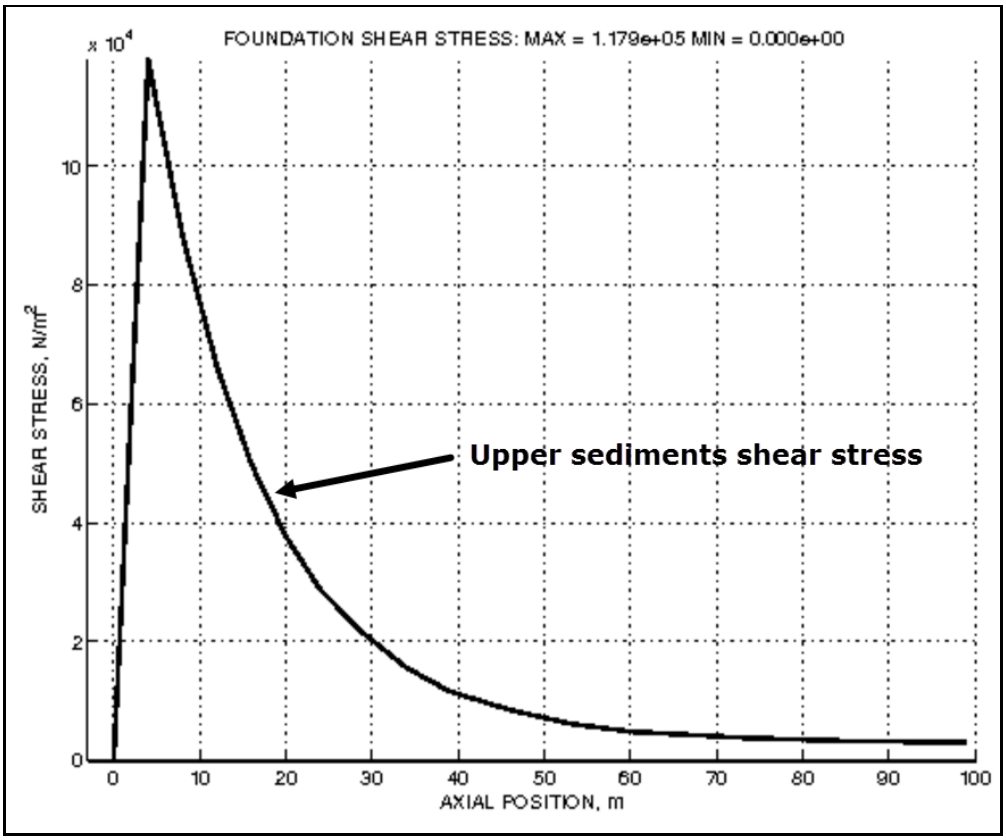

Fig. 13 Shear stresses in the upper foundation, if Tree/BOP is added without cementing (top)

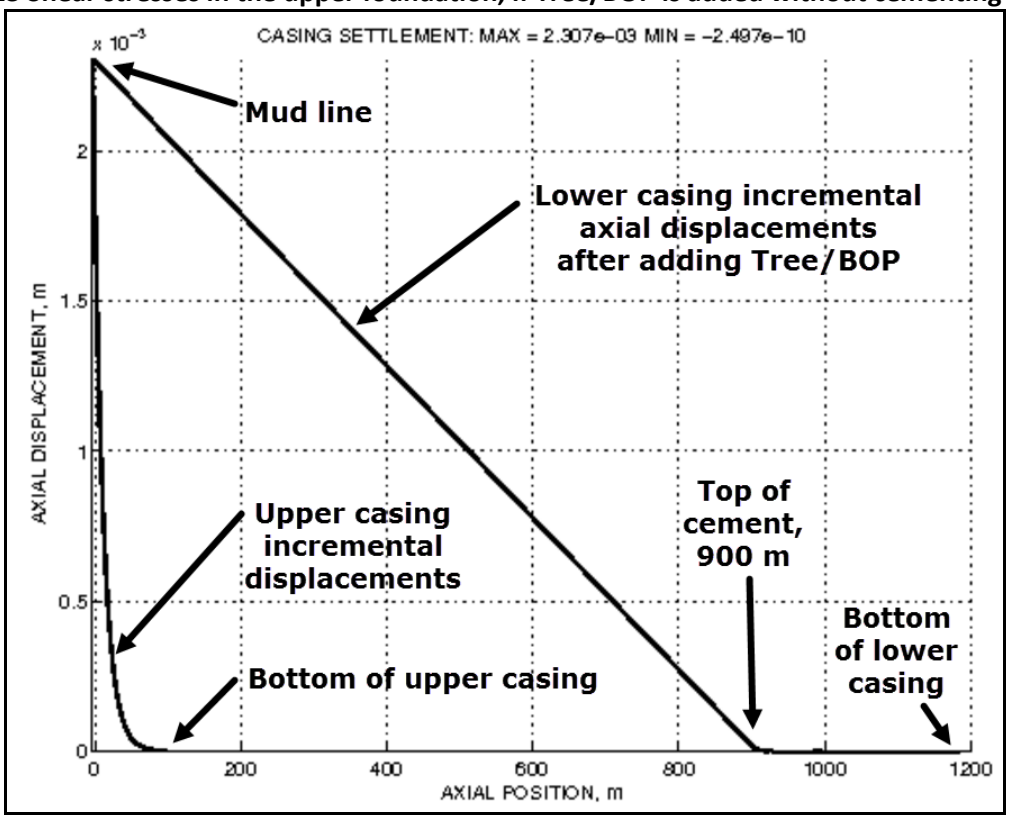

Fig. 14 Incremental displacements from the Tree/BOP weight, with cemented lower casing

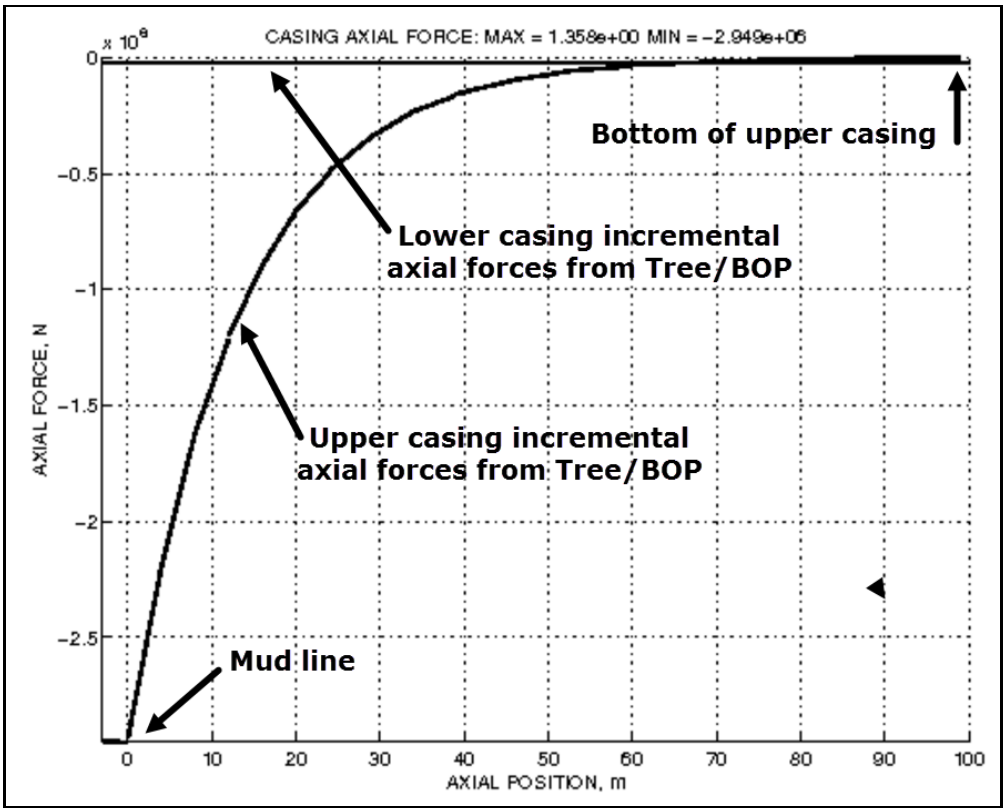

Fig. 15 Upper region incremental Tree/BOP compression forces in the casings